Canadian Conference - Pacific Conference on Earthquake Engineering 2023

Vancouver, British Columbia

June 25th – June 30th, 2023

Monitoring of the Recovery Process in Minami-Aso Village from the 2016 Kumamoto Earthquake based on Multi-Temporal Lidar Data

Fumio Yamazaki[1*] and Wen Liu[2]

[1]Research Fellow, National Research Institute for Earth Science and Disaster Resilience (NIED), Tsukuba, Japan
[2]Assistant Professor, Graduate School of Engineering, Chiba University, Chiba, Japan
[*]fumio.yamazaki@bosai.go.jp (Corresponding Author)

ABSTRACT

The use of multi-temporal LiDAR data was demonstrated for identifying damage to infrastructures and monitoring their recovery process in Minami-Aso village after the 16 April 2016 Kumamoto, Japan, earthquake. By taking the difference of digital surface models (DSMs) acquired at pre- and post-event times, landslides, bridge failures and collapsed buildings were extracted and the results were compared with field survey data and aerial optical images. From the co-event DSM difference, a large number of landslides were clearly identified and a settlement of road embankment connecting to the Choyo bridge was observed as well as many collapsed buildings. From the post-event 1.5-year DSM difference, the restoration of the Choyo bridge, removal of collapsed buildings, and slope stability works were monitored. From the LiDAR random point data acquired on November 2020, newly built Aso-Ohashi bridge with its high piers was observed clearly. Based on the multi-temporal LiDAR data, the recover process of infrastructures from the Kumamoto earthquake was monitored in the 3D form.

Keywords: the 2016 Kumamoto earthquake, landslide, bridge construction, recovery monitoring, LiDAR.

INTRODUCTION

Remote sensing is a useful tool to extract various damage situations in urban and rural areas from natural hazards [1]. Optical and Synthetic Aperture Radar (SAR) satellite sensors have been used frequently because pre- and post-event images covering affected areas are often available, and various change detection techniques have been applied for these images [2]. Change detection usually extracts two-dimensional (2D) changes in objects on the Earth surface. However, the damage situations of landslides, bridges, and buildings can be expressed more precisely by 3D changes [3]. To carry out 3D change detection, multi-temporal 3D models, in the form of digital elevation models (DEMs) are necessary. DEMs [4] are typically represented by a digital surface model (DSM), which includes trees and buildings, and a digital terrain model (DTM), in which those Earth surface objects have been removed from a DSM. DSMs with texture are usually produced through the stereo-matching of optical images [5, 6] from satellites or aircraft, or more recently by using Structure-from-Motion (SfM) techniques [7] for optical images [8, 9] obtained using unmanned aerial vehicles (UAVs).

A more direct way of generating DSMs is the use of airborne LiDAR (Light Detection and Ranging) data. The change detection of urban areas from multi-temporal LiDAR data was demonstrated first for ordinary (pre-disaster) times [10, 11]. The direct comparison of pre- and post-earthquake LiDAR data was conducted after the 2016 Kumamoto, Japan, earthquake with respect to crustal movement [12], building damage [13, 14], and landslides [15] in Mashiki town and its surrounding areas since the high-density pre-event data were available.

Remote sensing can also be used to monitor recovery and reconstruction processes after major disasters [16]. From very high-resolution optical images, the damage and reconstruction of Boumerdes city after the 2003 Algeria earthquake were investigated [17]. The urban recovery monitoring of Pisco city after the 2007 Pisco, Peru, earthquake [18] and that of Bam city, Iran, after the 2003 Bam earthquake [19] were carried out also using high-resolution optical images because they are easy to understand, and different satellite sensors can be used for long-term monitoring.

The authors obtained one pre-event and four post-event (April 2016 to November 2017) LiDAR data for Minami-Aso village, which was most severely affected by the 16 April 2016 Kumamoto earthquake [20, 21]. In the study [22], the extraction of collapsed buildings and the monitoring of their removal process were carried out. The building damage assessment results from the LiDAR DSMs were then compared with damage survey data by the municipal government [23].

Recently we acquired one more high-density LiDAR data observed in November 2020, 4.5-years after the Kumamoto earthquake. In this study, the extraction of damage to infrastructures is attempted and their recovery process is monitored by comparing the one pre-event and three post-event LiDAR data. The construction of the New Aso-Ohashi bridge is observed together with the restoration works of failed slopes and new building construction from the difference of the LiDAR DSMs. This paper highlights the use of multi-temporal LiDAR data for monitoring the recovery process in Minami-Aso village after the 2016 Kumamoto earthquake.

THE 2016 KUMAMOTO EARTHQUAKE AND MINAMI-ASO VILLAGE

A Mw6.2 earthquake hit the Kumamoto prefecture in Kyushu Island, Japan, on April 14, 2016 at 21:26 (JST), with the epicenter in the Hinagu fault at a shallow depth. Considerable structural damages and human casualties had been reported due to this event [21]. On April 16, 2016 at 01:25 (JST), 28 hours after the first event, another earthquake of Mw7.0 occurred in the Futagawa fault, closely located with the Hinagu fault. Thus, the first event was called as the "foreshock" and the second one as the "main shock". Extensive impacts due to strong shaking and landslides were associated by the Kumamoto earthquake sequence. A total of fifty (50) direct-cause deaths were accounted, mostly due to the collapse of wooden houses in Mashiki town [24] and landslides in Minami-Aso village [25].

Figure 1 shows the location of the causative faults and Japanese national GNSS Earth Observation Network System (GEONET) stations, operated by the Geospatial Information Authority of Japan (GSI), in the source area. The displacement of 75 cm to the east-northeast (ENE) was observed at the Kumamoto station while that of 97 cm to the southwest (SE) was recorded at the Choyo station in the main shock. These observations validated the right-lateral strike-slip mechanism of the Futagawa fault. Minami-Aso Village (area: 137.3 km^2, population: 11,500) is located in the western caldera of the Aso volcano. Figure 2 shows the on-site photos of the Minami-Aso village taken in our field survey in June 2016. The large landside, which caused the collapse of the Aso-Ohashi bridge, and ground failures including surface faulting and collapsed apartment buildings were seen in Kawayo district. Temporary housing units were under-construction near the Choyo GEONET station when we visited there.

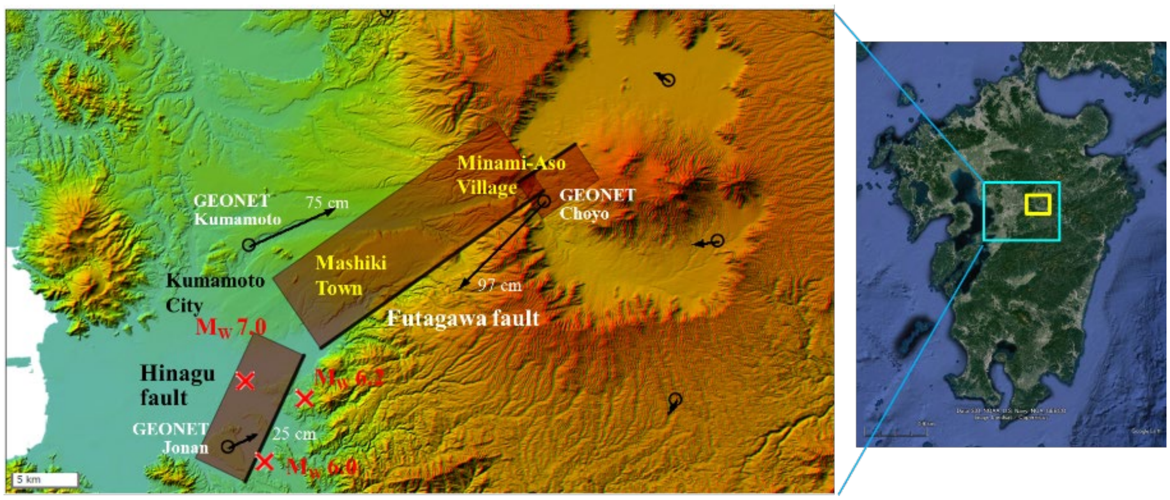

Figure 1. Location of causative faults and GNSS stations in the 2016 Kumamoto earthquake on a GSI map (left) and the extent of the left map (blue square) and Minami-Aso village (yellow square) in Kyushu Island (right).

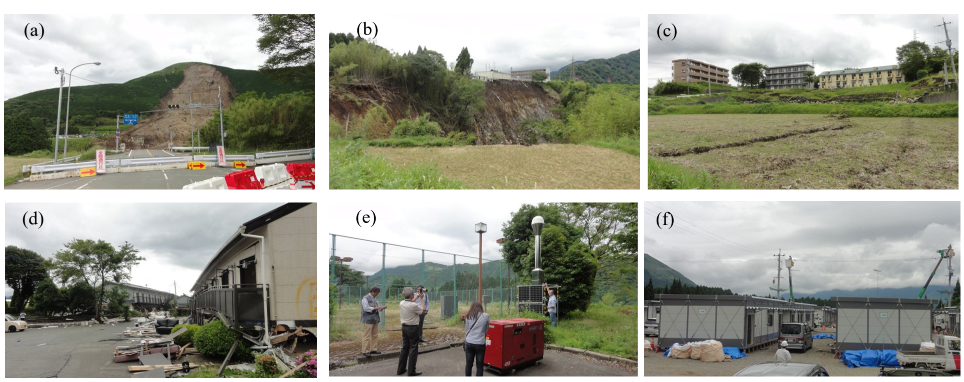

Figure 2. Damage situation of the Minami-Aso village on June 6, 2016; (a) the largest landslide in Tateno district, (b) a cliff-fall, (c) surface faulting and (d) collapsed apartment buildings in Kawayo district, (e) GEONET station, and (f) temporary housing units under construction in Choyo district.

The eastern edge of the causative fault [26] appeared on the ground surface in Kawayo and many wooden houses and apartment buildings were collapsed there. Tateno district was also severely affected by strong shaking and the failure of a water tank on the hill caused a mad-flow to the district. After the earthquake, the municipal government conducted the damage assessment for the all buildings of severely affected areas in Minami-Aso village based on the unified loss evaluation method of Japan [27, 28]. A total of 4,733 buildings were classified into five damage classes in terms of monetary loss [23].

Figure 3 shows a pre-event optical image of the study area, which includes the junction of the Kurokawa and Shirakawa rivers and surrounding heavily affected Kawayo and Tateno districts in Minami-Aso village.

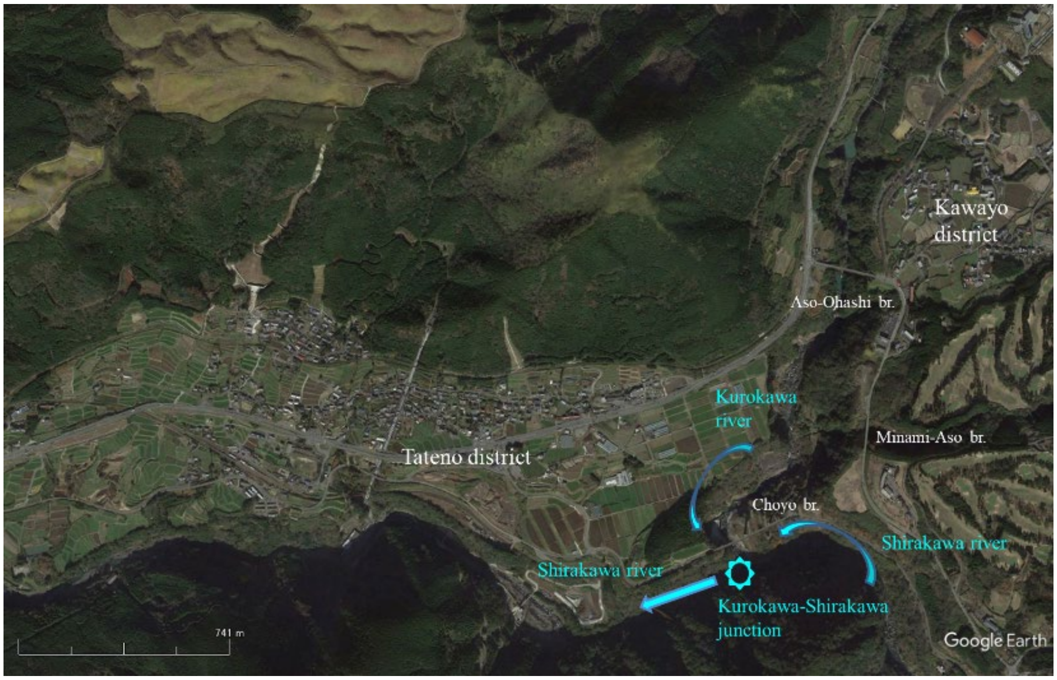

Figure 3. Pre-event optical image (2015/12/18) of Kawayo and Tateno districts in Minami-Aso village including the Kurokawa and Shirakawa river junction (Google Earth).

FOUR-TEMPORAL LIDAR DATA AND THEIR DSM DIFFERENCES

The pre- and post-event LiDAR data, shown in Table I and Figure 4, were used in this study. These datasets cover the north-western part of Minami-Aso village along the Shirakawa and Kurokawa rivers. The first three datasets were acquired by the GSI and the Ministry of Land, Infrastructure, Transport and Tourism (MLIT), Japan, for the purpose of national land surveying, disaster response, and river management. The 2020/11 LiDAR dataset was acquired by the Forestry Agency for assessing the earthquake impacts to the national forest in the Aso mountains.

The datasets contain original random points data as well as DTMs, where trees and buildings had been removed. Since our main objective is assessment of structural damage and recovery, we processed the original random point data and produced Digital Surface Models (DSMs) of 50-cm grid, including buildings and trees. Note that the average point densities of the current datasets (5 – 39 points/m^2) are much higher than those (1.5 – 4 points/m^2) used in our previous studies for Mashiki town [12,13].

Table 1. Acquisition date, average point density, DSM spacing, data owner, and corresponding optical images of the LiDAR datasets used in this study.

LiDAR Dataset Name	**a.** 2013/1	**b.** 2016/4	**c.** 2017/11	d. 2020/11
Acquisition Date (yr/mo/day)	2013/01/10–02/20	2016/04/19–23	2017/10/31–11/02	2020/10/26–12/1
Average Point Density (1/m^2)	5	11	39	18
DSM Spacing (cm)	50	50	25	50
Data Owner	MILT/GSI	GSI	MILT/GSI	Forestry Agency
Corresponding Aerial Image	Same time with LiDAR	2016/4/16, 29 GSI air photo	Same time with LiDAR	Same time with LiDAR

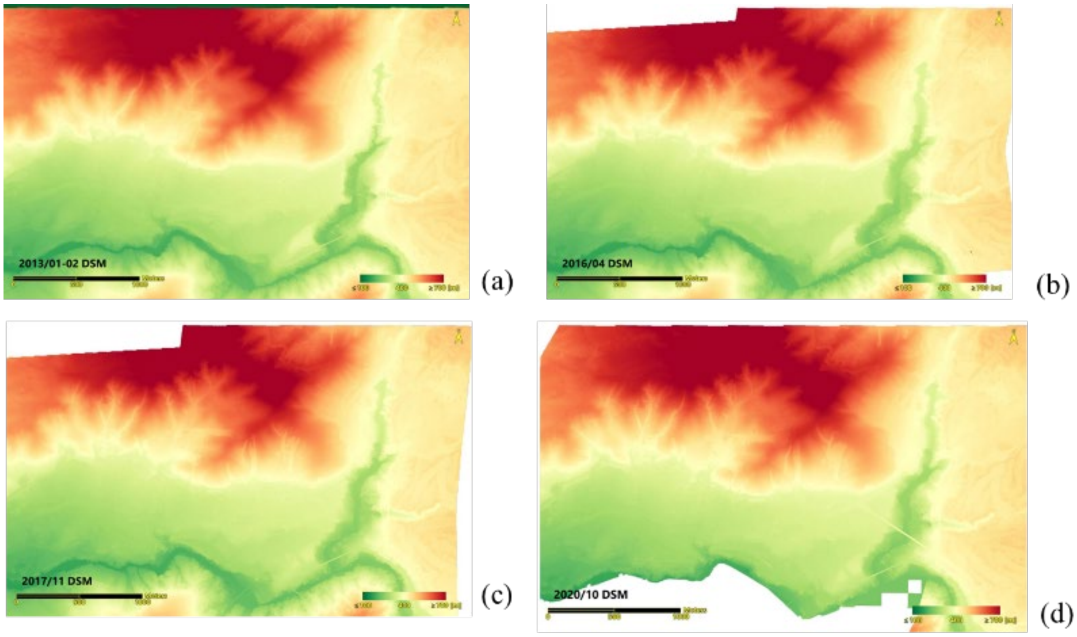

Figure 4. DSMs of the four LiDAR datasets for the study area of Mimami-Aso village.

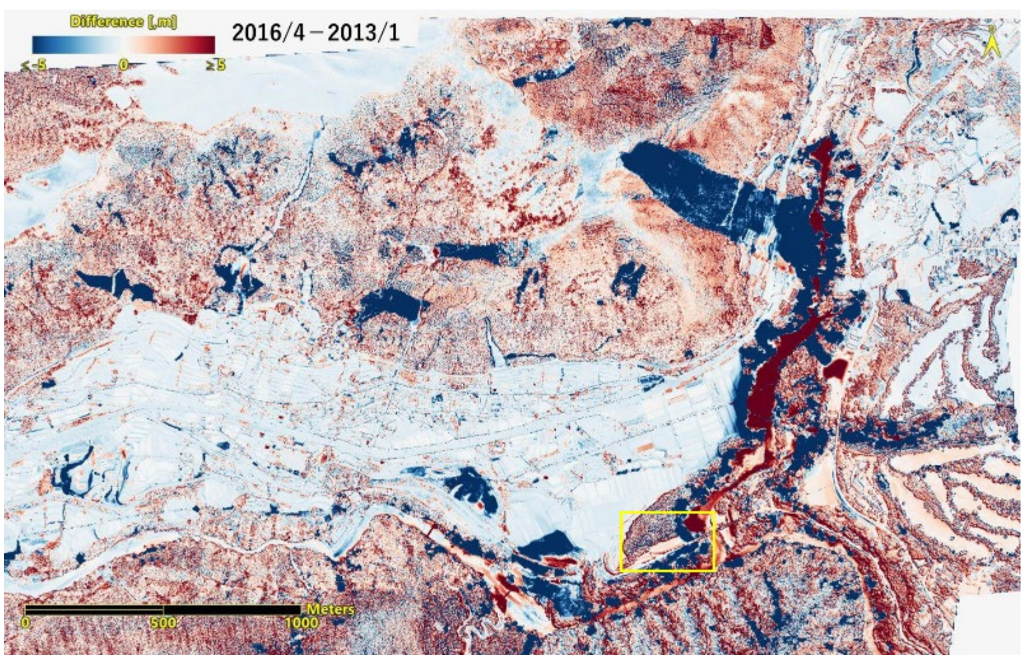

Figure 5. The DSM difference for the co-event period (2013/1 - 2016/4) of the study area.

The difference of DSMs between two acquisition periods is calculated by $\Delta H_{ij} = DSM_j - DSM_i$. Figure 5 shows the co-event DSM difference for the common area of the two datasets (a and b). The earthquake-induced landslides are clearly highlighted by the dark-blue color, showing the height reduction in the DSM by the main shock. Since large permanent ground displacements were observed in this area, we co-registered the pre- and post-event DSMs for each target area. The yellow square shows the area including the Choyo bridge, for a detailed investigation in the latter section.

Figure 6 shows the DSM difference for the common area of the datasets b and c. Since the difference corresponds to the post-event 1.5-year period, most landslides shown by the dark-blue color were caused by a heavy rain in June 2016, not due to the earthquake. The dark blue colored areas near the largest earthquake-induced landslide were recovery works for slope stability. The construction work of the foundations of the New Aso-Ohashi bridge is observed near the Kurokawa and Shirakawa river junction. Small blue spots in Kawayo and Tateno districts correspond to the removed damaged houses due to the earthquake [22].

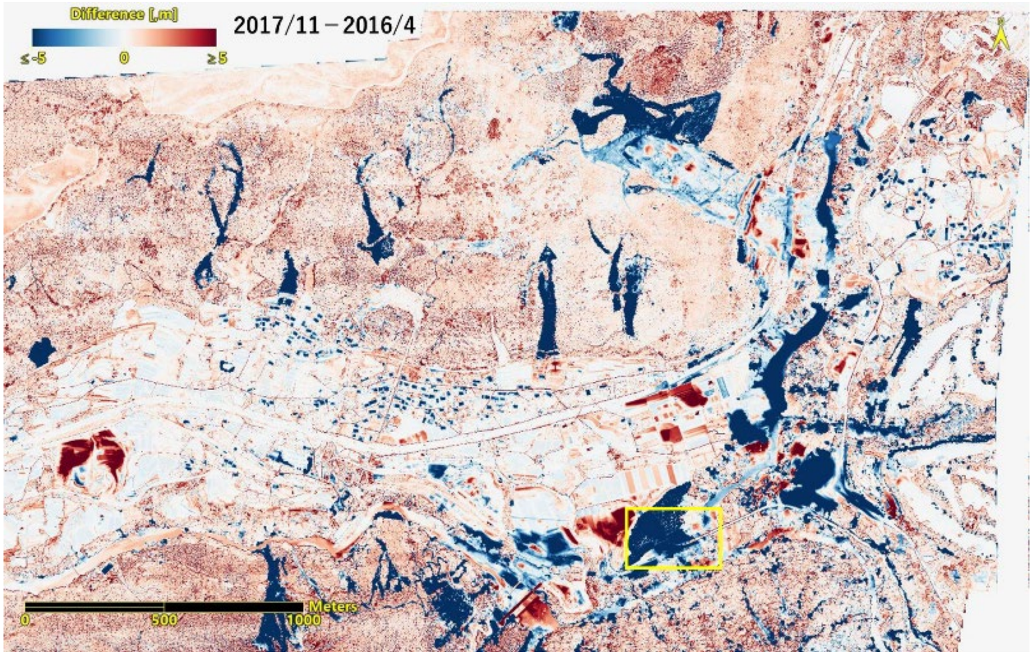

Figure 6. The DSM difference for the post-event period (2016/4 - 2017/11) of the study area.

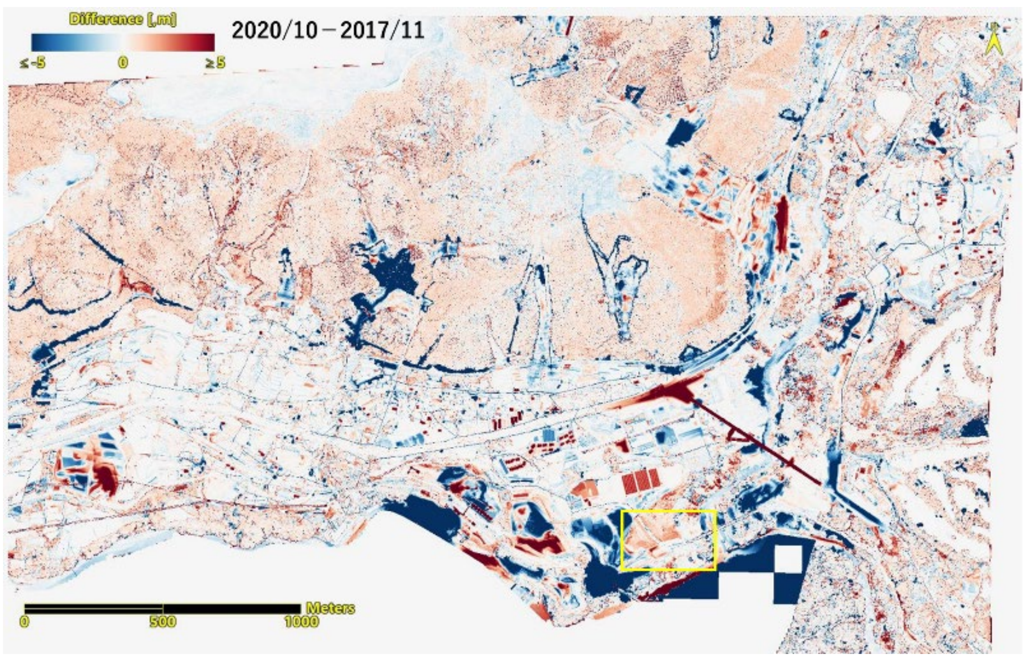

Figure 7. The DSM difference for the post-event period (2017/11 - 2020/10) of the study area.

Figure 7 shows the DSM difference for the common area of the datasets c and d in the recent post-event period. The thin red straight line shows the girder of the New Aso-Ohashi bridge, which opened for service in March 2021. Both the dark-blue color and red color (the height increase of the DSM) correspond to the construction works of roads, Tateno Dam and slope stability works. It is noticed that red spots corresponding to new construction of houses are observed in Tateno and Kawayo districts.

DAMAGE AND RECOVERY OF THE CHOYO BRIDGE

The Choyo bridge is a four-span prestressed concrete (PC) continuous girder bridge over the Kurokawa river close to the river junction. The total length is 276.0-m and the highest pier has 73-m height. Due to the earthquake, the west abutment subsided about 2 m and the east abutment sustained crack to its concrete wall [29, 30]. One of the three piers had serious cracks but the bridge was survived from the total collapse. The traffic was closed because the embankments of the two sides connecting to the bridge were failed and the asphalt on the road was crashed. Figure 8 shows the DSM differences and optical images showing damage and recovery of the Choyo bridge. From (a) and (c), the dark blue areas show slip-down parts of landslides and red areas are accumulated soils due to landslides. The settlement at the west abutment was calculated as 1.8 m from the DSM difference, which is close to the observed value, about 2 m [31] . From (b) and (d), dark-blue areas correspond to slope stability works to prevent further landslides to the roadway. It is noticed from the optical image that the western connecting road to the bridge was re-routed to construct new solid foundations of the bridge [31]. The route from Tateno to the Aso caldera through the Choyo bridge re-opened after finishing bridge repair and slope stability works in August 2017.

Figure 9 shows the 3D random point LiDAR data around the Choyo bridge observed in November 2020. The LiDAR data clearly shows the bridge girder, slope stability works, and even three piers as well as the valley and the river.

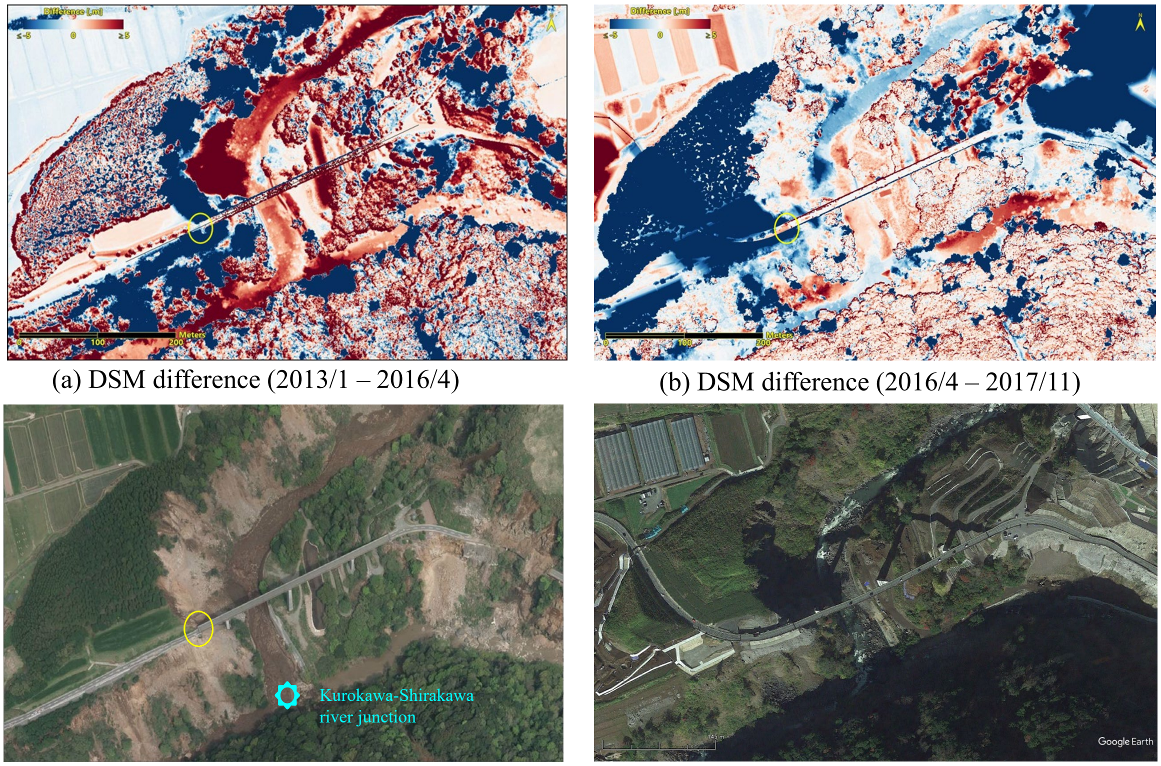

(a) DSM difference (2013/1 – 2016/4)

(b) DSM difference (2016/4 – 2017/11)

(c) Aerial image by GSI on 2016/04/16

(d) Aerial image from Google Earth on 2020/11/21

Figure 8. The DSM differences and optical images showing damage and recovery of the Choyo bridge

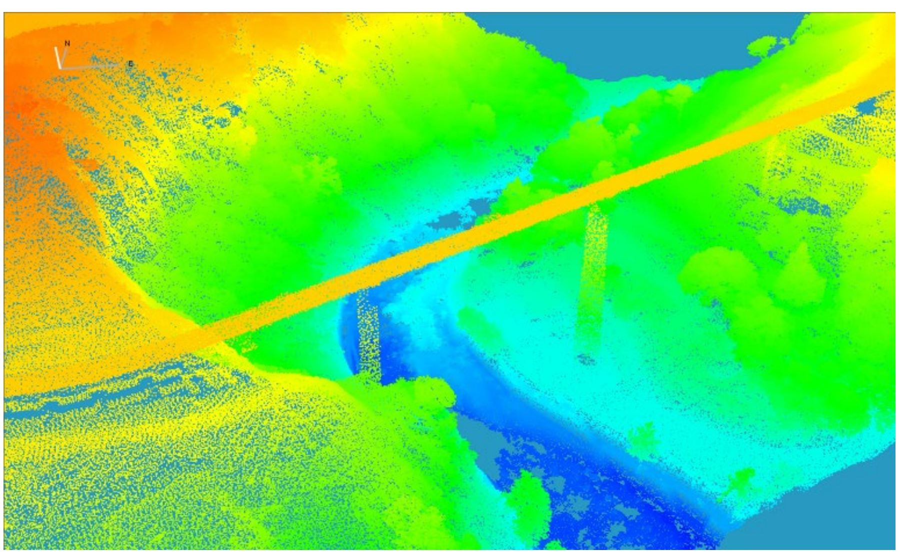

Figure 9. Oblique view of the 3D random point LiDAR data around the Choyo bridge in 2020/11

CONSTRUCTION OF THE NEW ASO-OHASHI BRIDGE

The collapsed Aso-Ohashi bridge was located at the junction between the national highway No. 57 (connecting Kumamoto and Oita prefectures) and the national highway No. 325 (leading to Takachiho town, Miyazaki prefecture). It was the most important route to the Aso caldera from Kumamoto city. Due the largest landslide caused by the main shock of the Kumamoto earthquake, the bridge was collapsed to the Kurokawa river and the route was closed almost 5 years after the earthquake. The New Aso-Ohashi bridge started its construction in March 2017, around one year after the earthquake, in about 600 m downstream of the collapsed bridge [32]. The new bridge is a three-span prestressed concrete (PC) continuous box-girder bridge with the total length 525 m and the highest pier 97 m. The new bridge opened for traffic on March 31, 2021, five years after the earthquake.

Figure 10 shows the DSM differences and optical images showing the construction of the New Aso-Ohashi bridge. From (a) and (c), the slop stabilization works of the river cliff were recognized to build the bridge piers and abutments. Filling works of the connecting road were also seen in red color. From (b) and (d), the bridge was seen to be almost completed together with the approach roads on November 2020. Figure 11 shows the 3D random point LiDAR data around the New Aso-Ohashi bridge observed in November 2020. The LiDAR data clearly exhibit the whole shapes of the bridges even three high piers, in spite of the vertical shouting scheme of laser pulses of airborne LiDAR. The top of the piers, however, cannot seen from the 3D plot since the laser pulses did not reach under the bridge girder.

Based on these observations, the multi-temporal LiDAR data are found to be quite useful to observe damage situations and recovery processes of infrastructures after natural disasters. We will use high-density LiDAR data to simulate Synthetic Aperture Radar (SAR) images of bridges [33, 34] for identifying bridge damage from natural disasters in the future.

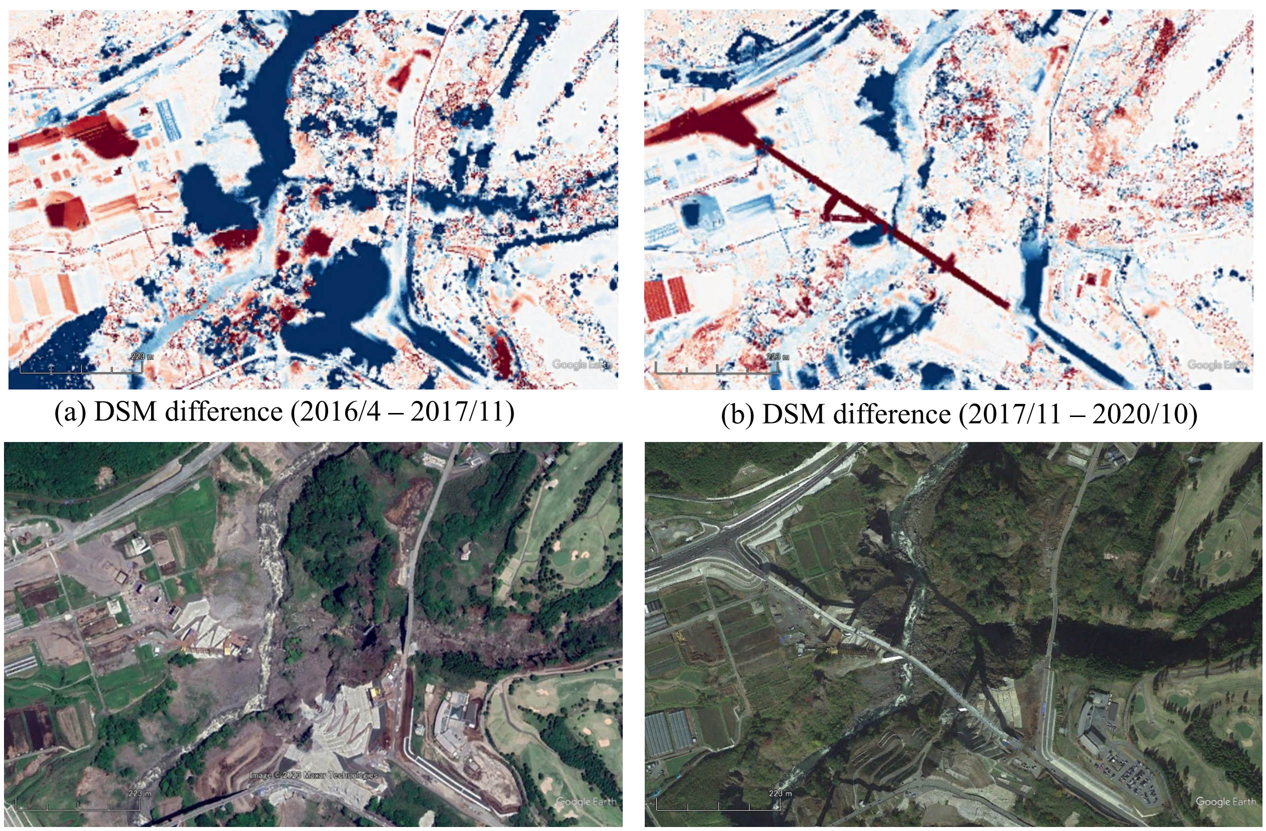

(a) DSM difference (2016/4 – 2017/11)

(b) DSM difference (2017/11 – 2020/10)

(c) Aerial image from Google Earth on 2018/05/10

(d) Aerial image from Google Earth on 2020/11/21

Figure 10. The DSM differences and optical images showing construction of the New Aso-Ohashi bridge

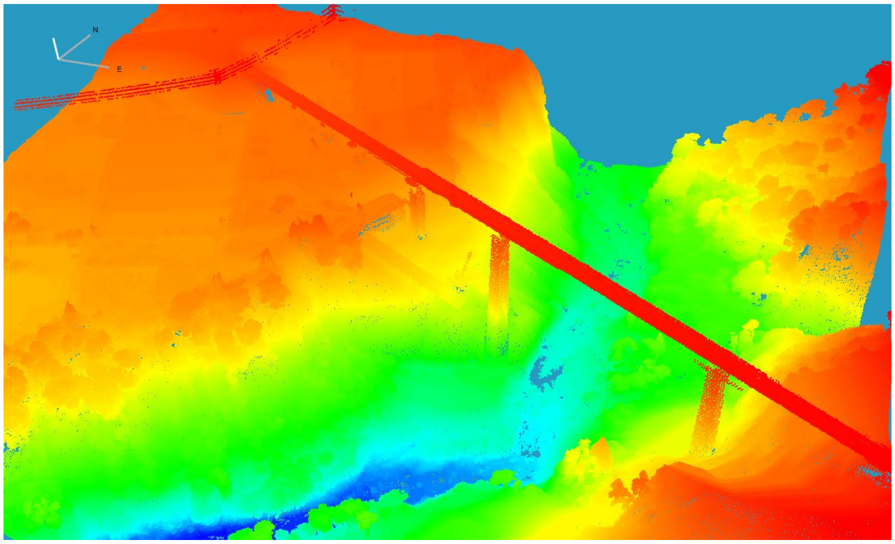

Figure 11. Oblique view of the 3D random point LiDAR data around the New Aso-Ohashi bridge in 2020/11

FIELD SURVEY OF MINAMI-ASO VILLAGE AND UAV FLIGHTS

For gathering the damage and reconstruction information of Minami-Aso village from the 2016 Kumamoto earthquake, the authors have conducted field surveys of the affected area a total of six times (2016/06/6-7, 07/3-4, 08/8-9, 2021/07/21, 2021/12/23-24, 2022/12/4-5). We flew a UAV (DJI Phantom 4) over some affected areas in the survey during 2016/08/8-9 [9]. In the field survey during 2021/12/23-24, we also flew a very small UAV (DJI Mini 2, 199 g) form off-road open space. Figure 12 shows aerial images recorded by a 4K camera, taken from the UAV at the altitude about 30-50 m [25]. (a) shows the restoration works of the largest landslide and the reconstructed national highway No. 57 in Tateno district. (b) shows an overview of Kawayo district, where the collapsed Aso-Ohashi bridge still exists. The newly constructed Aso-Ohashi bridge in (c) and the repaired Choyo bridge in (d). Aerial surveys from UAVs are considered to be quite useful to monitor the recovery process of wide areas.

(a) Slope stability works for the largest landslide

(b) Kawayo district and collapsed Aso-Ohashi bridge

(c) Completed New Aso-Ohashi bridge

(d) Choyo bridge and New Aso-Ohashi bridge (back)

Figure 12. UAV photos in our field survey on 2021/12/23

CONCLUSIONS

This study investigates the use of multi-temporal LiDAR data for identifying damage to infrastructures and monitoring their recovery process in Minami-Aso village after the 2016 Kumamoto, Japan, earthquake. The difference of digital surface models (DSMs) acquired at one pre-event (2013) and three post-event (2016, 2017, 2020) times were calculated and landslides, bridge failures and collapsed buildings were extracted from them. From the co-event DSM difference, a large number of landslides were clearly identified and collapsed buildings were extracted, comparing with field survey data and aerial optical images. A 1.8-m settlement of the west abutment was observed for the Choyo bridge as well as many surrounding landslides. From the post-event 1.5-year DSM difference, the restoration of the Choyo bridge, removal of collapsed buildings, and the slope stability works were monitored. From the Lidar random point data acquired on November 2020, the newly built Aso-Ohashi bridge was observed clearly including its high piers. The UAV images in our field surveys also confirmed the recovery process of infrastructures in the Minami-Aso area. This study highlighted the usefulness of multi-temporal LiDAR data, not only extracting the damage status of infrastructures but also monitoring the recover process from natural disasters in the three-dimensional form.

ACKNOWLEDGMENTS

The three-temporal LiDAR datasets used in this study were provided by the GSI and the latest LiDAR data were provided from the Forestry Agency through agreement with the National Research Institute for Earth Science and Disaster Resilience (NIED). This research was partially supported by JSPS KAKENHI Grant Number 21H01598, Japan.

REFERENCES

[1] Rathje, E., Adams, B.J. (2008). "The role of remote sensing in earthquake science and engineering: Opportunities and challenges." *Earthquake Spectra*, 24, 471–492.
[2] Dong, L., Shan, J.A. (2013). "Comprehensive review of earthquake-induced building damage detection with remote sensing techniques." *ISPRS Journal of Photogrammetry and Remote Sensing*, 84, 85–99.
[3] Qin, R., Tian, J., Reinartz, P. (2016). "3D change detection – Approaches and applications." *ISPRS Journal of Photogrammetry and Remote Sensing*, 122, 41–56.
[4] Štular, B., Lozić, E., Eichert, S. (2021). "Airborne LiDAR-Derived Digital Elevation Model for Archaeology." *Remote Sensing*, 13, 1855.
[5] Maruyama, Y., Tashiro, A., Yamazaki, F. (2014). "Detection of collapsed buildings due to earthquakes using a Digital Surface Model constructed from aerial images." *Journal of Earthquake and Tsunami*, 8(1).
[6] Susaki, J. (2015). "Region-based automatic mapping of tsunami-damaged buildings using multi-temporal aerial images." *Natural Hazards*, 76, 397–420.
[7] Cheng, M.L., Matsuoka, M., Liu, W., Yamazaki, F. (2022). "Near-real-time gradually expanding 3D land surface reconstruction in disaster areas by sequential drone imagery." *Automation in Construction*, 135, 104105.
[8] Fernandez Galarreta, J., Kerle, N., Gerke, M. (2015). "UAV-based urban structural damage assessment using object-based image analysis and semantic reasoning." *Natural Hazards and Earth System Sciences*, 15, 1087–1101.
[9] Yamazaki, F., Kubo, K., Tanabe, R., Liu, W. (2017). "Damage assessment and 3D modeling by UAV flights after the 2016 Kumamoto, Japan earthquake." In *Proceedings of 2017 IEEE International Geoscience and Remote Sensing Symposium*, Fort Worth, TX, USA, 3182–3185.
[10] Vu, T.T., Matsuoka, M., Yamazaki, F. (2004). "LIDAR-based change detection of buildings in dense urban areas." In *Proceedings of 2004 IEEE International Geoscience and Remote Sensing Symposium*, Anchorage, AK, USA, 3413–3416.
[11] Xu, H., Cheng, L., Li, M., Chen, Y., Zhong, L. (2015). "Using Octrees to detect changes to buildings and trees in the urban environment from airborne LiDAR data." *Remote Sensing*, 9682–9704.
[12] Moya, L., Yamazaki, F., Liu, W., Chiba T. (2017). "Calculation of coseismic displacement from lidar data in the 2016 Kumamoto, Japan, earthquake." *Natural Hazards and Earth System Sciences*, 17, 143–156.
[13] Moya, L., Yamazaki, F., Liu, W., Yamada, M. (2018). "Detection of collapsed buildings from lidar data due to the 2016 Kumamoto earthquake in Japan." *Natural Hazards and Earth System Sciences*, 18, 65–78.
[14] Hajeb, M., Karimzadeh, S., Matsuoka, M. (2020). "SAR and LIDAR datasets for building damage evaluation based on Support Vector Machine and Random Forest algorithms—a case study of Kumamoto Earthquake, Japan." *Applied Sciences*, 10, 8932.
[15] Liu, W., Yamazaki, F., Maruyama, Y. (2019). "Detection of earthquake-induced landslides during the 2018 Kumamoto Earthquake using multitemporal airborne Lidar data." *Remote Sensing*, 11, 2292.
[16] Ghaffarian, S., Kerle, N., Filatova, T. (2018). "Remote sensing-based proxies for urban disaster risk management and resilience: a review." *Remote Sensing*, 10, 1760.
[17] Meslem, A., Yamazaki. F., Maruyama, Y., Benouar, D., Kibboua, A., Mehani, Y. (2012). "The effects of building characteristics and site conditions on the damage distribution in Boumerdes after the 2003 Algeria earthquake." *Earthquake Spectra*, 28(1), 185–216.

[18] Hoshi, T., Murao, O., Yoshino, K., Yamazaki, F., Estrada, M. (2014). "Post-disaster urban recovery monitoring in Pisco after the 2007 Peru earthquake using satellite image." *Journal of Disaster Research*, 9(6), 1059-1068.

[19] Hashemi-Parast, S.O., Yamazaki, F., Liu, W. (2017). "Monitoring and evaluation of the urban reconstruction process in Bam, Iran, after the 2003 Mw6.6 earthquake." *Natural Hazards*, 85(1), 197-213.

[20] Geospatial Information Authority of Japan (GSI). (2016). "Information on the 2016 Kumamoto Earthquake." http://www.gsi.go.jp/BOUSAI/H27-kumamoto-earthquake-index.html

[21] Yamazaki, F., Liu, W. (2016). "Remote sensing technologies for post-earthquake damage assessment: A case study on the 2016 Kumamoto earthquake." In *Proceedings of the 6th Asia Conference on Earthquake Engineering*, Cebu City, Philippines.

[22] Yamazaki, F., Liu, W., Horie, K. (2022). "Use of multi-temporal LiDAR data to extract collapsed buildings and to monitor their removal process after the 2016 Kumamoto earthquake." *Remote Sensing*, 14, 5970.

[23] Minami-Aso Village Government (2022). "Recovery report from the 2016 Kumamoto Earthquake." https://www.vill.minamiaso.lg.jp/kiji0031924/3_1924_up_pykdezn3.pdf (in Japanese).

[24] Liu, W., Yamazaki, F. (2017). "Extraction of collapsed buildings due to the 2016 Kumamoto earthquake based on multi-temporal PALSAR-2 data." *Journal of Disaster Research*, 12(2), 241-250.

[25] Yamazaki, F., Liu, W. (2022). "Recovery monitoring of Minami-Aso area after the 2016 Kumamoto earthquake based on remote sensing data." In *Proceedings of the 8th Asia Conference on Earthquake Engineering*, Taipei, Taiwan, 1171-1178, ISBN: 20978-986-89629-5-8.

[26] Shirahama, Y., Yoshimi, M., Awata, Y. et al. (2016). "Characteristics of the surface ruptures associated with the 2016 Kumamoto earthquake sequence, central Kyushu, Japan." *Earth Planets and Space*, 68(1).

[27] Cabinet Office of Japan. (2018). "Operational guideline for damage assessment of residential buildings in disasters." http://www.bousai.go.jp/taisaku/pdf/h3003shishin_all.pdf (in Japanese).

[28] Tanaka, S., Shigekawa, K. (2014). "Development of training system for building damage assessment using actual buildings." *Journal of Disaster Research*, 9(2), 188–197.

[29] National Institute for Land and Infrastructure Management (NILIM) (2017). "Report on Damage to Infrastructures by the 2016 Kumamoto Earthquake." *Technical Note of NlLIM No. 967*, http://www.nilim.go.jp/lab/bcg/siryou/tnn/tnn0967.htm (in Japanese).

[30] Japan Society of Civil Engineers (JSCE) (2017). "Report on damage survey and investigation following the 2016 Kumamoto earthquake." Earthquake Damage Survey Series No. 1, JSCE Committee on Earthquake Engineering (in Japanese).

[31] Sawada, M., Imamura, T., Nakagawa, R., Hoshikuma, J. (2018). "Restoration and monitoring of a PC rigid-frame bridge damaged by the Kumamoto Earthquake." *Civil Engineering Journal*, 60(2), 36-39 (in Japanese).

[32] Fujikawa, S., Ubayashi, Y., Ishibashi, R. (2020). "Rebuilding method of Aso Ohashi Bridge affected by Kumamoto Earthquake in 2016." *Civil Engineering Journal*, 62(12), 28-31 (in Japanese).

[33] Liu, W., Maruyama, Y., Yamazaki, F. (2021). "Detection of collapsed bridges from multi-temporal SAR intensity images by machine learning techniques." *Remote Sensing*, 13, 3508.

[34] Yamazaki, F., Liu, W. (2022). "Extraction of bridge damage in the 2016 Kumamoto earthquake using airborne SAR data." In *Selected papers from the Lifelines 2022 Conference*, Los Angeles, USA, 546-555.